A Context-Aware Cognitive SIMO DL Transceiver for LTE HetNet Enhanced Pico-Cell Range Expansion

Imen Mrissa, Faouzi Bellili, Sofiène Affes, and Alex Stéphenne
INRS-EMT, 800 De La Gauchetiere Ouest, Suite 6900, Montreal (Quebec), H5A 1K6, Canada.
Emails: {mrissa, bellili, affes}@emt.inrs.ca and stephenne@ieee.org

***Abstract*—Deploying small cells (pico-cells and femto-cells) or relays in a macro-cell network is a promising solution to increase system capacity. However, due to their very low transmit powers, small cells are prone to severe interference corruption from macro-cells. Moreover, Users Equipment (UEs) are offloaded to small cells only if the latter guarantee a better received signal powers. Hence, interference problems make pico-cells covering range very small, the range expansion (RE) technique was specifically conceived to overcome this problem. The basic idea is to bias the received signal power from pico-cells in such a way that more UEs are offloaded from the macro-cell than the real case. In order to enhance the performance of the RE technique, we design in this paper a new single-input multiple-output (SIMO) context-aware cognitive transceiver (CTR) that is able to switch to the best performing modem in terms of link-level throughput. On the top of conventional adaptive modulation and coding (AMC), we allow the context-aware CTR to make best selection among three different pilot-utilization modes: conventional data-aided (DA) or pilot-assisted, non-DA (NDA) or blind, and NDA with pilot which is a newly proposed hybrid version between the DA and NDA modes. We also enable the CTR to make best selection between two different channel identification schemes: conventional least-squares (LS) and newly developed maximum-likelihood (ML) estimators. Depending on whether pilot symbols can be properly exploited or not at the receiver, we further enable the new CTR to make best selection among two data detection modes: coherent or differential. It will be seen that using our new cognitive transceiver on LTE Heterogeneous Network (HetNet) jointly with the range expansion technique leads to a considerable gains reaching, respectively, 48% and 42% for 5^{th} percentile cell-site and average cell-site throughput.**

I. Introduction

The increasing demand of mobile radio services causes a bottleneck challenge for all wireless communication systems. Deploying Heterogeneous Networks (HetNets) has been envisaged in order to resolve this issue which exacerbated with the limited frequency resources. The basic concept of a HetNet network is to integrate low-power and reduced range nodes (known as small cells) in a macro-cell layout. Small cells provide additional radio resources and hence guarantee a cost-effective system capacity and throughput improvement. However, the interference issue is the major obstacle for efficient small cell's operation due to their weak transmission power (pico-cell's transmit power is 40 times smaller than that of macro-cell). This entails the following two major problems: $i)$ mobile user equipment (UE) switches to the small-cell only if it experiences a better received signal power and $ii)$ low throughput performance as UEs served by small-cells suffer from low SINR level due to interference issue. Range Expansion (RE) technique is a very promising solution for problem $i)$ and enhances HetNet system capacity by offloading more users to the pico-cells. In the literature, many solutions are proposed to mitigate interference problems for RE technique and enhance system performances for HetNet systems using RE technique [1], [2], [3], [4], and [5]. The basic idea behind RE is to bias the signal power received by the mobile UE from the small-cell so that more users are assigned to it. Having problem $i)$ fixed by RE technique, our goal in this paper is to cope with problem $ii)$ and enhance system-level DL-LTE throughput in heterogeneous networks (HetNets). We develop a new CTR that provides considerable throughput gains for both macro- and especially pico-cells. Most interestingly, when applied with RE, the new CTR offers significant throughput gains achieving 48% and 42% for 5^{th} percentile cell-site and average cell-site throughput respectively. Note here that interference mitigation is beyond the scope of this work and that we assume a co-channel pico-cell deployment. The remainder of this paper is structured as follows. In Section II, we introduce the context-aware CTR modes along with the different channel estimation schemes. In Section III, exhaustive computer simulations are presented and discussed in order to assess and illustrate the tremendous performance gains of the newly proposed CTR. Finally, concluding remarks are drawn out in Section IV.

Work supported by the CREATE PERSWADE <www.create-perswade.ca> and the Discovery Grants Programs of NSERC and a Discovery Accelerator Supplement (DAS) Award from NSERC.

II. Context-aware cognitive transceiver modes

A. DA or pilot-assisted mode

Pilot symbols are reference (i.e., known) symbols inserted according to a predefined mapping as training sequences for channel estimation and synchronization purposes.

1) LS channel estimator: This conventional estimator uses pilot symbols to estimate the channel by minimizing the squared difference between the received signal and the known pilot symbols. Let $y_{i,\text{DA}}$ denote the received signal on pilot sub-carrier i among N_{pilot} pilot sub-carriers at the OFDM pilot symbol index t. For convenience, we will henceforth omit the time index t. The transmitted pilot symbol $x_{i,\text{DA}}$ is related to $y_{i,\text{DA}}$ as follows:

$$y_{i,\text{DA}} = h_i x_{i,\text{DA}} + n_i \qquad i = 0, 1, ..., N_{\text{pilot}} - 1, \tag{1}$$

where h_i is the complex channel coefficient and n_i is a zero-mean Gaussian noise. The matrix notation of (1) is given by:

$$\mathbf{y}_{\text{DA}} = \mathbf{X}_{\text{DA}}\mathbf{h} + \mathbf{n}, \tag{2}$$

where $\mathbf{X}_{\text{DA}} = \text{diag}\left\{x_{0,\text{DA}}, x_{1,\text{DA}}, \ldots, x_{N_{\text{pilot}}-1,\text{DA}}\right\}$, $\mathbf{h} = [h_0, h_1, ..., h_{N_{\text{pilot}}-1}]^T$, and $\mathbf{n} = [n_0, n_1, ..., n_{N_{\text{pilot}}-1}]^T$ is the i.i.d complex zero-mean Gaussian noise vector. The LS algorithm aims at minimizing $(\mathbf{y}_{DA} - \mathbf{X}_{DA}\mathbf{h})^\dagger(\mathbf{y}_{\text{DA}} - \mathbf{X}_{\text{DA}}\mathbf{h})$ ($\dagger$ denotes matrix Hermitian transpose) to estimate the channel frequency response thereby leading to [6]:

$$\widehat{\mathbf{h}}_{\text{LS}} = \mathbf{X}_{\text{DA}}^{-1}\mathbf{y}_{\text{DA}}, \tag{3}$$

where $\mathbf{A}^{-1}$ denotes the matrix inverse. The estimates for the channel coefficients at non-pilot subcarriers can then be easily obtained by interpolation [9]. However, when the channel is fast fading (i.e., high user velocity), the pilot symbols spacing may not be sufficient to enable proper tracking of the channel variations. Moreover, increasing pilot overhead leads to a throughput decrease which is not desirable for any communication system.

2) ML estimator: Here, we consider the ML channel estimator developed in [7]. For each OFDM symbol, the DA ML estimator captures the channel's time variations via a polynomial-in-time expansion of order $(J-1)$. In fact, the channel over each $\{r^{th}\}_{r=1}^{N_r}$ antenna branch and the i^{th} subcarrier, in a SIMO system, is modeled as follows [8]:

$$h_{i,r}(t_n) = \sum_{j=0}^{J-1} c_{i,r}^{(j)} t_n^j + REM_J^{(i,r)}(t_n). \tag{4}$$

978-1-4673-6555-0/15/$31.00 ©2015 IEEE

Here, $t_n = nT_s$ with T_s being the sampling period. The polynomial order $J-1$ is a Doppler-dependent parameter optimized in [7]. Moreover, $c_{i,r}^{(j)}$ is the j^{th} coefficient of the channel polynomial approximation over the i^{th} sub-carrier and the r^{th} branch. As will be explained shortly, the term $REM_J^{(i,r)}(t_n)$ refers to the remainder of the Taylor series expansion which can be driven to zero by choosing an approximation window of sufficiently small size thereby yielding the following accurate approximation [7]:

$$h_{i,r}(t_n) = \sum_{j=0}^{J-1} c_{i,r}^{(j)} t_n^j. \tag{5}$$

Channel estimation is performed independently over each pilot sub-carrier. For the sake of simplicity, we also omit the sub-carrier index in the remainder of this paper.

To use a small model order $J-1$ in (4) and thereby avoid costly inversions of large-size matrices, the new DA ML estimator partitions the whole observation window into K local approximation windows of the same size. Then, it maximizes the probability density function (pdf) of the locally-observed vectors, $\mathbf{y}_{\text{DA}}^{(k)}$, parametrized by $\mathbf{c}_k$:

$$p(\mathbf{y}_{\text{DA}}^{(k)};\mathbf{c}_k|\mathbf{B}_k) = \frac{1}{(2\pi\sigma^2)^{N_{\text{DA}}N_r}} \exp\Big\{-\frac{1}{2\sigma^2}\big[\mathbf{y}_{\text{DA}}^{(k)}-\mathbf{B}_k\mathbf{c}_k\big]^H\big[\mathbf{y}_{\text{DA}}^{(k)}-\mathbf{B}_k\mathbf{c}_k\big]\Big\}, \tag{6}$$

where $\mathbf{c}_k$ is a vector containing the unknown approximation polynomial coefficients over the k^{th} approximation window (i.e., for all the antenna branches) defined as $\mathbf{c}_k = [\mathbf{c}_{k,1}^T, \mathbf{c}_{k,2}^T, ..., \mathbf{c}_{k,N_r}^T]^T$ with $\mathbf{c}_{k,r} = [c_{k,r}^{(0)}, c_{k,r}^{(1)}, ..., c_{k,r}^{(J-1)}]^T$ where $c_{k,r}^{(j)}$ is the j^{th} coefficient of the channel polynomial approximation over the i^{th} sub-carrier, the k^{th} approximation window and the r^{th} branch and σ^2 defines the noise variance. In (6), $\mathbf{y}_{\text{DA}}^{(k)} = [\mathbf{y}_{1,\text{DA}}^{(k)}\, \mathbf{y}_{2,\text{DA}}^{(k)} \cdots \mathbf{y}_{N_r,\text{DA}}^{(k)}]^T$ with $\mathbf{y}_{r,\text{DA}}^{(k)}$ being the received pilot samples over the antenna element r within the k^{th} approximation window, i.e., $\mathbf{y}_{r,\text{DA}}^{(k)} = [y_r^{(k)}(t_1)\, y_r^{(k)}(t_2) \ldots y_r^{(k)}(t_{P_{\text{DA}}})]$. Here P_{DA} is the number of pilot symbols in each approximation window which is covering N_{DA} pilot and non-pilot received samples. The approximation window size N_{DA} is another Doppler-dependent design parameter optimized in [7]. Moreover $\mathbf{B}_k$ is a $P_{\text{DA}}N_r \times JN_r$ block-diagonal matrix defined as $\mathbf{B}_k = \text{blkdiag}\{\mathbf{A}_k\mathbf{T}, \mathbf{A}_k\mathbf{T}, ..., \mathbf{A}_k\mathbf{T}\}$. Here, $\mathbf{A}_k$ is the $P_{\text{DA}} \times P_{\text{DA}}$ diagonal matrix of the transmitted pilot symbols within the k^{th} observation window, i.e., $\mathbf{A}_k = \text{diag}\{a_k(t_1), a_k(t_2), ..., a_k(t_{P_{\text{DA}}})\}$, and $\mathbf{T}$ is a Vandermonde matrix given by:

$$\mathbf{T} = \begin{pmatrix} 1 & t_1 & ... & t_1^{J-1} \\ 1 & t_2 & ... & t_2^{J-1} \\ \vdots & \vdots & \ddots & \vdots \\ 1 & t_{P_{DA}} & ... & t_{P_{DA}}^{J-1} \end{pmatrix}. \tag{7}$$

The estimate of the channel coefficients over all the receiving antenna branches are obtained by setting the partial derivative of (6) [or its natural logarithm] to zero yielding:

$$\widehat{\mathbf{c}}_{k,\text{DA}} = (\mathbf{B}_k^\dagger \mathbf{B}_k)^{-1}\mathbf{B}_k^\dagger \mathbf{y}_{\text{DA}}^{(k)}, \tag{8}$$

from which the DA ML estimates for the channel coefficients at both pilot and non-pilot positions are obtained by injecting the estimates of the polynomial coefficients established in (8) back into (4).

B. NDA with pilot or hybrid mode

Ensuring reliable communications is the purpose of all wireless communication systems. However, receiver mobility and surrounding scatterers' motion make channel estimation accuracy a truly challenging task. For that reason, pilot symbols that are inserted far apart, in the time-frequency grid, do not enable accurate tracking of fast-varying channels. Information carried in data symbols is hereafter exploited in a hybrid channel identification scheme in order to enhance the system performance.

1) NDA w. pilot RLS estimator: At OFDM symbol $t+1$, we use preceding transmitted signals as a training sequence of t symbols. In fact, the channel estimate, $\widehat{\mathbf{H}}_{t+1}$, at OFDM symbol $t+1$ is obtained using the weighted LS method as follows [10]:

$$\widehat{\mathbf{H}}_{t+1} = \underset{\widehat{\mathbf{H}}}{\text{argmin}} \sum_{w=1}^{t} \beta_w \|\mathbf{y}_w - \widehat{\mathbf{H}}\mathbf{Q}_w x_w\|^2, \tag{9}$$

where the channel variation $\mathcal{H}$ is approximated to the D^{th} order Taylor series expansion according to the OFDM symbol instance m, i.e.: $\mathcal{H}_w \simeq \sum_{d=0}^{D} w^d \mathcal{H}^{<d>} = \mathbf{H}\mathbf{Q}_w$ with $\mathbf{Q}_w \triangleq [w^0\mathbf{I}_{N_r}, w^1\mathbf{I}_{N_r}, ..., w^D\mathbf{I}_{N_r}]^T \in \mathbb{R}^{N_r(D+1)\times N_r}$. In (9) $\beta_w \in \mathbb{R}$ stands for a weighting coefficient given by $\beta_w = \lambda^{t-w}$ where $\lambda \in \mathbb{R}$ is referred to as a forgetting factor. The exponential weighted RLS algorithm is implemented as follows:

$$\begin{aligned} \boldsymbol{\zeta}_t &= \boldsymbol{\Phi}_{t-1}^{-1}\mathbf{Q}_t x_t \in \mathbb{C}^{N_r(D+1)\times 1}, \\ \alpha_t &= \frac{1}{\lambda + \boldsymbol{\zeta}_t^\dagger \mathbf{Q}_t x_t} \in \mathbb{R}, \\ \boldsymbol{\Phi}_t^{-1} &= \lambda^{-1}\boldsymbol{\Phi}_{t-1}^{-1} - \lambda^{-1}\alpha_t \boldsymbol{\zeta}_t \boldsymbol{\zeta}_t^\dagger \in \mathbb{C}^{N_r(D+1)\times N_r(D+1)}, \\ e_t &= y_t - \widehat{\mathbf{H}} x_t \in \mathbb{C} \\ \widehat{\mathbf{H}}_{t+1} &= \widehat{\mathbf{H}}_t + \alpha_t e_t \zeta_t^\dagger \in \mathbb{C}^{1\times N_r(D+1)}. \end{aligned}$$

For initialization, $\widehat{\mathbf{H}}_1$ is considered to be identically zero and $\boldsymbol{\Phi}_0^{-1}$ is set to $\varrho\mathbf{I}_{N_r(D+1)}$ where $\varrho \gg 1$ is a constant with sufficiently large value. Moreover, x_1 is assumed to be a pilot symbol. The channel estimate $\widehat{\mathbf{H}}_{t+1}$ is then used to detect the $(t+1)^{th}$ symbol x_{t+1}.

2) NDA w. pilot ML estimator: We consider the expectation maximization (EM) based ML estimator developed in [7]. The new estimator uses pilot and data symbols jointly in order to track the channel variations. In a first step and for a given sub-carrier, the NDA with pilot estimator relies on pilot symbols to estimate the channel coefficients at pilot OFDM symbols as described in Section II-A2. In a second step, the NDA with pilot estimator applies the EM algorithm over all the received samples in order to jointly estimate the channel coefficients and detect the transmitted unknown symbols at non-pilot positions as well. The iterative EM based ML algorithm runs in two main steps and uses as initialization $\widehat{\mathbf{c}}_{k,\text{DA}}$ obtained in (8) from pilot positions only.

• Expectation step (E-Step):

During the E-Step, the pdf function defined in (6) takes into account all the possible transmitted symbols $\{a_m\}_{m=1}^M$ where M is the modulation order. In fact, at each iteration q, for every approximation window of size N_{NDA} symbols, the objective function is updated as follows:

$$\begin{aligned} Q(\mathbf{c}_k \mid \widehat{\mathbf{c}}_k^{(q-1)}) &= -N_{\text{NDA}}N_r \ln(2\pi\sigma^2) \\ &- \frac{1}{2\sigma^2}\sum_{r=1}^{N_r}\left(M_{2,k}^{(r)} + \sum_{n=1}^{N_{\text{NDA}}} \alpha_{n,k}^{(q-1)} |\mathbf{c}_{r,k}^T \mathbf{t}(n)|^2 - 2\beta_{r,n,k}^{(q-1)} \mathbf{c}_{r,k}\right), \end{aligned} \tag{10}$$

where $M_{2,k}^{(r)} = E\{|y_{r,k}(n)|^2\}$ is the second-order moment of the received samples over the r^{th} antenna branch, $\mathbf{t}(n) = [1, t_n, t_n^2, ..., t_n^{J-1}]^T$ and:

$$\alpha_{n,k}^{(q-1)} = \sum_{m=1}^{M} P_{m,n,k}^{(q-1)} |a_m|^2, \tag{11}$$

$$\beta_{r,n,k}^{(q-1)}(\mathbf{c}_{r,k}) = \sum_{m=1}^{M} P_{m,n,k}^{(q-1)} \Re\{y_{r,k}^{*}(n) a_m \mathbf{t}^T(n) \mathbf{c}_{i,k}\}. \quad (12)$$

Here, $P_{m,n,k}^{(q-1)} = P(a_m \mid \mathbf{y}_k(n); \widehat{\mathbf{c}}^{(q-1)})$ is the *a posteriori* probability of a_m at iteration $(q-1)$ that is computed using the Bayes' formula as follows:

$$P_{m,n,k}^{(q-1)} = \frac{P(a_m) P\left(\mathbf{y}_k(n) | a_m; \widehat{\mathbf{c}}_k^{(q-1)}\right)}{P\left(\mathbf{y}_k(n); \widehat{\mathbf{c}}_k^{(q-1)}\right)}. \quad (13)$$

Since the symbols are assumed to be equally likely transmitted, we have $P(a_m) = \frac{1}{M}$ and therefore:

$$P\left(\mathbf{y}_k(n); \widehat{\mathbf{c}}_k^{(q-1)}\right) = \frac{1}{M} \sum_{m=1}^{M} P\left(\mathbf{y}_k(n) | a_m; \widehat{\mathbf{c}}_k^{(q-1)}\right). \quad (14)$$

• Maximization step (M-Step):

During the M-Step, the objective function obtained in (10) is maximized with respect to $\mathbf{c}_k$:

$$\widehat{\mathbf{c}}_k^{(q)} = \underset{\mathbf{c}_k}{\operatorname{argmax}}\, Q(\mathbf{c}_k | \widehat{\mathbf{c}}_k^{(q-1)}), \quad (15)$$

yielding the following more refined estimates for the approximation polynomial coefficients, i.e.:

$$\widehat{\mathbf{c}}_{r,k}^{(q)} = \left(\sum_{n=1}^{N_{\text{NDA}}} \mathbf{t}(n) \mathbf{t}^T(n) \right)^{-1} \sum_{n=1}^{N_{\text{NDA}}} \lambda_{r,n,k}^{(q-1)} \mathbf{t}(n). \quad (16)$$

In (16), $\lambda_{r,n,k}^{(q-1)}$ is given by:

$$\lambda_{r,n,k}^{(q-1)} = \left[\widehat{a}_k^{(q-1)}(t_n) \right]^{*} y_{r,k}(t_n), \quad (17)$$

in which

$$\widehat{a}_k^{(q-1)}(t_n) = \sum_{m=1}^{M} P_{m,n,k}^{(q-1)} a_m, \quad (18)$$

is the soft symbol estimate at iteration $q-1$ and $\mathbf{t}(\text{n}) = [1, t_n, t_n^2, ..., t_n^{J-1}]^T$.

C. NDA or blind mode

For blind or NDA channel estimation, no pilot symbols are exploited by the receiver. Channel estimation is performed based on the information carried by all symbols assumed unknown a priori. Phase ambiguity is resolved by differential modulation. The blind RLS channel estimator algorithm is already the one described in Section II-B1. However, an arbitrary guess of the first sent symbol is used to initialize the recursive algorithm. The blind channel estimation algorithm is also the one described in Section II-B2. The only difference here, however, is that the initialization is arbitrary and random.

D. Data detection modes

On the top of selecting the appropriate channel estimator and pilot-use couples among DA ML, NDA w. pilot ML, NDA ML, DA LS, NDA w. pilot RLS and NDA RLS, the new context-aware CTR selects one of the following data detection modes:

- Coherent if pilot symbols are used.
- Non coherent or differential if no pilot symbols are used. We also implement a "fully differential" transceiver version for which no channel estimation is required and where data detection is based on differential modulation-demodulation only. We use the soft-decision-aided DAPSK detection algorithm developed in [11] and [12].

III. Simulation setup and results

A 1×2 antenna configuration (1 transmit antenna at the eNodeB and 2 receive antennas at the mobile) is adopted as a SIMO configuration example for discussion in the rest of this paper. In the following, exhaustive computer simulations will be conducted in order to assess the performance of the newly proposed CTR transceiver at both the link- and system-levels.

A. Link-level simulations

In this subsection, link-level simulations assuming only one base station and a single mobile UE are used to draw decision rules regarding:

1) The best channel identification mode [among DA, NDA w. pilot (i.e., hybrid), and completely NDA] that yields the highest link-level throughput.
2) The best detection scheme between coherent and differential depending on whether pilot symbols can be properly exploited or not at the receiver, respectively.
3) The best modulation-coding CQI couple among the conventional coherent (CQI-C) and the newly-designed differential (CQI-D) ones.

The decision rules are drawn out against the operating conditions in terms of SNR, channel model type, mobile speed, and CQI value. Most significant LTE DL link-level parameters are summarized in Tab. I.

TABLE I. Link-level simulations parameters.

Number of User Equipments	1
Channel bandwidth (MHz)	15
Carrrier frequency (GHz)	2.1
Frame duration (ms)	10
Subframe duration (ms)	1
Number of resource blocks	75
Number of subcarriers/RB	12
OFDM symbols per subframe	7
Transmit mode	SIMO
Channel types	PedA, VehA, and VehB
Channel coding	Convolutional turbo encoder

We consider a Pedestrian A (PedA) flat-fading channel model for users with mobile speed of 2 km/h and Vehicular A (VehA) and B (VehB) frequency-selective channels for users with mobile speeds of 30 km/h and 100 km/h. Their power delay profiles (PDPs) are given in [16].
In order to account for adaptive modulation and coding (AMC), a CQI value indicates to the eNodeB the modulation order and the channel coding rate adopted in each subframe. The CQI value ranges between 1 and 15 defining, respectively, six, three, and six possible coding rates for QPSK/DQPSK, 16QAM/D16Star-QAM, and 64QAM/D64Star-QAM modulations [15]. Note that CQI-C and CQI-D stand for coherent and differential detection modulations, respectively. In our simulations, the CQI values as well as the SNR are assumed to be perfectly known at the receiver side. Assessment of CQI feedback and delay errors are beyond the scope of this contribution.
We define three different CTRs depending on the implemented channel estimation algorithms. The first proposed CTR (denoted hereafter as "CTR LS") switches between the fully differential mode and the different LS channel estimation schemes: namely DA LS, NDA w. pilot LS, and NDA LS. The second proposed CTR referred as "CTR ML" switches between the fully differential detection mode and the different ML channel estimation schemes: namely DA ML, NDA w. pilot ML, and NDA ML. The third CTR is a smarter cognitive transceiver, denoted hereafter simply as "CTR" is able to switch between all the detection modes and channel estimation schemes listed previously for both CTR ML and CTR LS. Fig. 1 depicts the link-level throughput gains of the CTR with respect to the conventional non-cognitive

transceiver that applies the DA LS channel estimator regardless of the channel conditions [1]. The gains are presented for each triplet (channel type, mobile speed, SNR/CQI value) and our benchmark is the DA LS as it is the conventional used channel estimation mode. A seen from Fig. 1, the proposed CTR offers tremendous link-level throughput gains over the conventional DA LS transceiver that operates with no cognition at all. For instance, in the low SNR region, such throughput gain can be as high as 700% for VehB channels and mobile speed of 100 kmph.

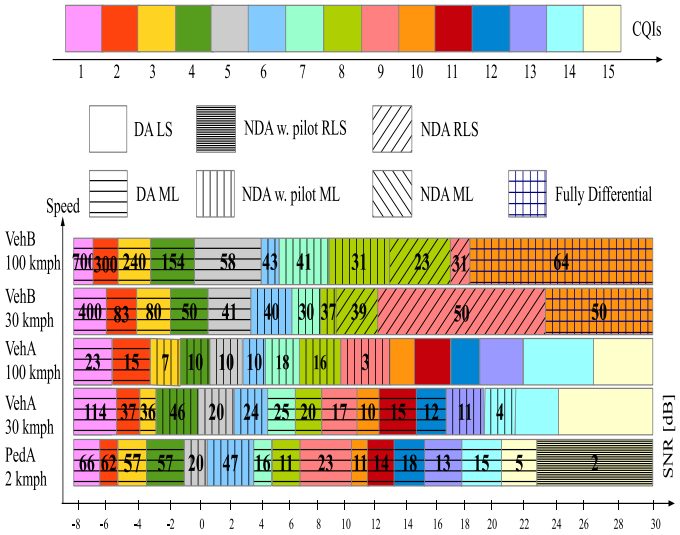

Fig. 1. Decision rules of the proposed CTR and the throughput gain percentages against the conventional DA LS receiver (with coherent detection) versus SNR for different channel types and mobile speeds.

B. System-level simulations

The link-level-based decision rules, identified in the previous subsection, are then assigned to a HetNet LTE DL system-level simulator in order to assess the performance of the new cognitive transceiver under more realistic conditions that take into account the interference effects of all network elements. Our goal is to enhance the network-wide system performance and especially to improve pico-cells efficiency since they are able to provide considerable capacity improvements while transmitting with weaker powers (40 times weaker than transmitted power from macro-cells as shown in Tab. II). We simulate a DL LTE-HetNet with 7-hexagonal-cell network with pico-cells being dropped randomly in each macro area. We consider a low clustering UEs distribution where 4 UEs are dropped in each hotspot (pico-cell area) and the others are dropped uniformly over the whole cell-site area. Each UE selects its serving cell(i.e., macro or pico) by comparing the corresponding received signal power. Since pico-cells transmit a much weaker power than the hosting macro-cell UEs tend to select the latter as the serving cell in most of cases (i.e., very rare UEs offloading to pico-cells). Range Expansion is a solution that has been introduced to increase the number of UEs that are served by pico-cells. The idea is to bias the signal power received by the mobile UE from the small cells so that more UEs are connected to them and thereby increasing their coverage area. It is worth noting here that UEs that are offloaded to small cells by RE technique still suffer from a serious interference problem since the required RE bias value tend to be sufficiently high in order to compensate the high received power for the macro-cell. As will be seen shortly, when used in conjunction with RE, the proposed CTR reduces the effect of this interference problem and as such expands pico-cells' serving range. To see this, we simulate

[1]Note here that link-level throughput gains for CTR-LS and CTR-ML are not shown due to space limitations. Their performance will, however, be assessed later when RE will be used as well.

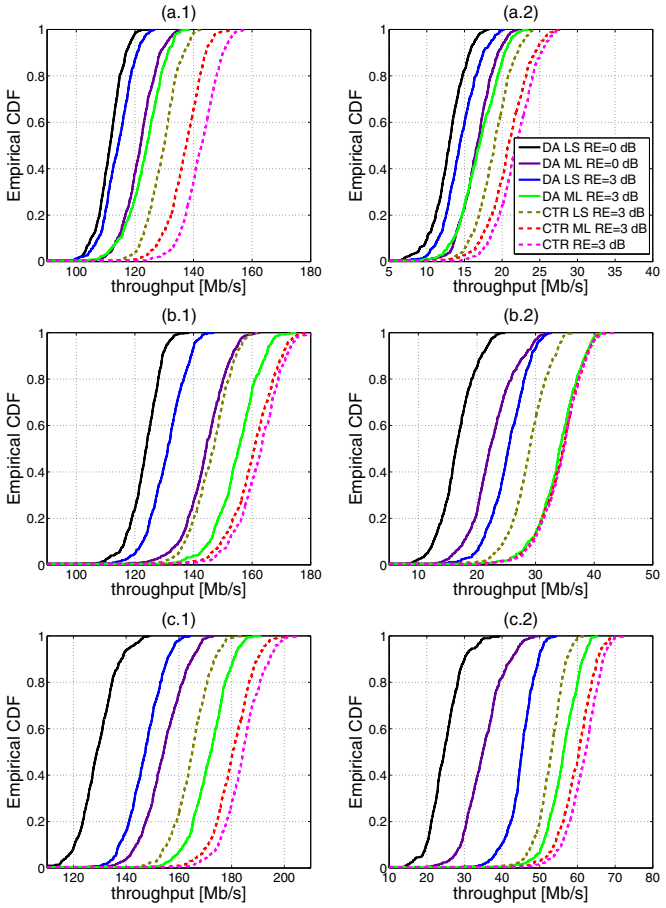

Fig. 2. System-level throughput empirical CDF for a) 1 pico-cell per macro area, b) 2 pico-cells per macro area, c) 4 pico-cells per macro area; 1) per cell-site, and 2) per pico-cell.

a co-channel pico-cell deployment where macro- and pico-cells share the same radio resources (interference mitigation is beyond the scope of this work). An exhaustive list of the system-level parameters we used during our simulations is provided in Tab. II. We also assume that 50% of the users move with a speed of 2

TABLE II. SYSTEM-LEVEL SIMULATION PARAMETERS.

Inter-site distance	500 meters
Path loss model	TS 36.942, subclause 4.5.2
Antenna pattern	macro:3-dimensional/pico:Omnidirectional
Shadowing	Log-normal with 10 dB standard deviation
Maximum macro-BS TX power	46 dBm
Scheduling algorithm	Proportional Fair
Minimum distance between pico pNodeBs	40 meters
Maximum pico-DS TX power	30 dBm
Number of UEs per cell-site	60

kmph and experience a PedA channel type. Moreover, 30% and 20% of the users are assumed to have a speed of 30 and 100 kmph, respectively. Medium and high speed users experience a VehA channel type and we simulate $\{1, 2, 4\}$ pico-cells in each macro area as defined in [14]. Fig. 3-(a) reveals that the number of UEs assigned to pico-cells increases with the number of dropped pico-cells per cell-site and with the RE bias level. Fig. 3-(b), however, shows that adding more pico-cells and/or increasing RE bias level leads to pico-users' SINR degradation due to the aforementioned interference effect. For a given RE bias level and number of dropped pico-cells, our goal is to enhance pico-cells performance by applying the different versions of our newly proposed CTR. Fig. 2 shows that our new CTRs (i.e., CTR-LS and CTR-ML and CTR), jointly with RE, enhance considerably the throughput CDFs for the pico-cells and the whole cell-site as compared to the conventional non-cognitive DA LS (with and without RE). Fig. 4 shows the absolute average throughput for pico-cells and

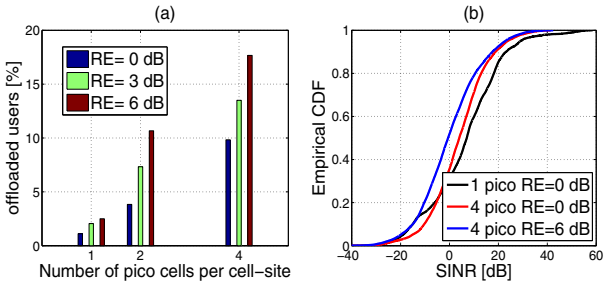

Fig. 3. (a) Percentage of offloaded users to PeNBs (b) Empirical CDF of pico-cell user's SINR.

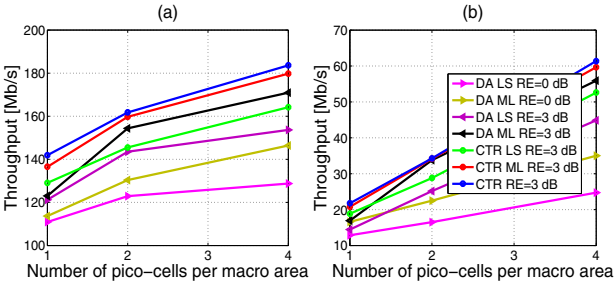

Fig. 4. System-level throughput : a) per cell-site and b) per pico-cell.

the whole cell-site. It is seen that when applying our CTR to the RE technique the throughput performances are notably improved compared to RE with no cognition. Average and 5^{th} percentile (i.e., cell-edge) throughput gains are shown in Fig. 5. It is seen that, in presence of 4 picocells per cell-site, the new CTR along with RE technique offers an average pico-cells throughput gain as high as 150% versus 80% for RE without cognition. The cell-edge gain provided by our CTR can also reach a gain as high as 250% versus a gain of 130% for RE without cognition. Regarding the whole cell-site, our CTR also achieves an average and cell-edge throughput gains exceeding 40% compared to about 15% only when applying RE without cognition.

IV. Conclusion

In this paper, we developed a new SIMO context-aware transceiver (CTR) that is able to switch to the best performing modem in terms of link-level throughput. On the top of conventional adaptive modulation and coding (AMC), we allow the new CTR to make best selection among three different pilot-utilization modes: conventional (DA) or pilot-assisted, non-DA (NDA) or blind, and NDA with pilot which is a newly proposed hybrid version between the DA and NDA modes. We also enable the proposed CTR to make best selection between two different channel identification schemes: conventional least-square (LS) and newly developed maximum-likelihood (ML) estimators. Depending on whether pilot symbols can be properly exploited or not at the receiver, we further enable the CTR to make best selection among two data detection modes: coherent or differential. Owing to extensive and exhaustive simulations on the downlink (DL) of a long-term evolution (LTE) heterogeneous network (HetNet), we are able to draw out the decision rules of the new CTR that identify the best combination triplet of pilot-use, channel-identification, and data-detection modes to achieve the best link-level throughput at any operating condition in terms of channel type, mobile speed, signal-to-noise ratio (SNR), and channel quality indicator (CQI). The new CTR achieves remarkable average and cell-edge throughput gains as compared to the conventional no-cognitive DA LS transceiver. In fact, we can reach a cell-edge throughput gain as high as 48% comparing to only 17% when applying RE without cognition for the case of 4 dropped pico-cells.

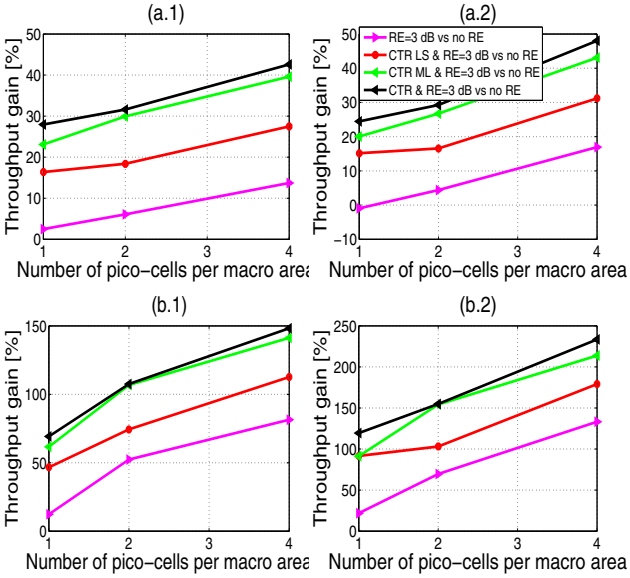

Fig. 5. System-level throughput gains: a) per cell-site, and b) per pico-cell; with 1) average, and 2) cell-edge.

References

[1] R. Madan, J. Borran, A. Sampath, N. Bhushan, A. Khandekar, and J. Tingfang, "Cell association and interference coordination in heterogeneous LTE-a cellular networks," *IEEE JSAC*, vol. 28, no. 9, pp. 1479-1489 Dec. 2010.

[2] A. Kamal, V. Mathai, A novel cell selection method for LTE HetNet *IEEE ICCSP*, pp. 738-742 April 2014.

[3] K. Okino, T. Nakayama, C. Yamazaki, H. Sato, Y. Kusano, "Pico cell range expansion with interference mitigation toward LTE-advanced heterogeneous networks," in *Proc. ICC Workshops*, Japan, June 2011, pp. 1-5.

[4] K. Kikuchi, H. Otsuka, H. "Proposal of adaptive control CRE in heterogeneous networks," in *Proc IEEE 23rd PIMRC*, 2012.

[5] S. Strzyz, K.I. Pedersen, J. Lachowski, F. Frederiksen, "Performance optimization of pico node deployment in LTE macro cells," in *IEEE FutureNetw*, 2011.

[6] J.-J. Van de Beek *et al* "On channel estimation in OFDM systems," in *Proc. IEEE 45th VTC.*, 1995, vol. 2, pp. 815-819.

[7] F. Bellili, R. Meftehi, S. Affes, and A. Stéphenne, "Maximum likelihood SNR estimation of linearly-modulated signals over time-varying flat-fading SIMO channels," *IEEE TSP.*, vol. 63, no. 2, pp. 441-456. Jan. 2015.

[8] P. Bello, "Characterization of randomly time-variant linear channels," *IEEE TCOM.*, vol. 11, no. 4, pp. 360-393, Dec. 1963.

[9] S. Omar , A. Ancora, and D.T.M. Slock, "Performance analysis of general pilot-aided linear channel estimation in LTE OFDMA systems with application to simplified MMSE schemes," in *Proc IEEE 19th PIMRC*, 2008.

[10] T.K. Akino, "Optimum weighted RLS channel estimation for rapid fading mimo channels," *IEEE TWireless.*, vol. 7, no. 11, pp. 4248-4260, Nov. 2008.

[11] D. D. Liang, S. X. Ng. Soon, and L. Hanzo, "Soft-decision star-QAM aided BICM-ID," *IEEE SPL.*, vol. 18, no. 3, pp. 169-172, Mar. 2011.

[12] C. Xu, D. Liang, S. X. Ng, and L. Hanzo, "Reduced-complexity noncoherent soft-decision-aided DAPSK dispensing with channel estimation," *IEEE TVT.*, vol. 62, no. 6, pp. 2633- 2643, July 2013.

[13] 3GPP Standard TS 36.211 V8.2.0 (2008-03).

[14] 3GPP TR 36.814 V9.0.0

[15] 3GPP TS 36.213 V8.8.0 Release 8 (2009-10)

[16] R. Jain, "Channel Models: A tutorial," *WiMAX forum AATG*, Ferbruray 2007.